

Phase-sensitive time-modulated surface plasmon resonance polarimetry for wide dynamic range biosensing

P. P. Markowicz, W. C. Law, A. Baev, P. N. Prasad

Institute for Lasers, Photonics and Biophotonics, Department of Chemistry, State University of NY at Buffalo, 430 NSC Building, Buffalo, NY 14260

S. Patskovsky, A. V. Kabashin

Engineering Physics Department, École Polytechnique de Montréal, C. P. 6079, succ. Centre-Ville, Montréal (Québec), Canada, H3C 3A7
sergiy.patskovsky@polymtl.ca

Abstract: A novel polarimetry scheme is proposed to improve the performance of phase-sensitive Surface Plasmon Resonance (SPR) biosensors. The scheme uses s-polarized light, not affected by SPR, as a reference beam, while information on the phase of the p-polarized component is obtained from an analysis of phase-polarization state of light of mixed polarization. We utilize temporal modulation of the beam reflected under SPR by a photo-elastic modulator and show that, under certain birefringent geometry, the signals at the 2nd and 3rd harmonics of modulated frequency can provide ultra-sensitive phase-based response to changes of the refractive index (thickness) of thin films on gold. We also show that the proposed configuration significantly improves detection limit compared to conventional intensity-sensitive SPR, yet enables to maintain wide dynamic range of measurements, which is normally difficult with phase-sensitive SPR schemes. Biosensing applications of the proposed scheme are illustrated in a biological model reaction of avidin – biotin binding on gold.

©2007 Optical Society of America

OCIS codes: (120.5050) Instrumentations, measurement, and metrology; (240.6680) Optics at surfaces.

References and links

1. Paras N. Prasad, *Introduction to Biophotonics*, Wiley-Interscience (2003).
2. B. Liedberg, C. Nylander, I. Lundstrom, "Biosensing with surface plasmon resonance - how it all started," *Biosens. Bioelectron.* **10**, i-ix (1995).
3. P. Schuck, "Use of surface plasmon resonance to probe the equilibrium and dynamic aspects of interactions between biological macromolecules," *Annu. Rev. Biophys. Biomol. Struct.* **26**, 541-566 (1997).
4. P.B. Garland, "Optical evanescent wave methods for the study of biomolecular interactions," *Q. Rev. Biophys.* **29**, 91-117 (1996).
5. E. Kretschmann, H. Raether, "Radiative decay of non radiative surface plasmons excited by light," *Z. Naturforschung A* **23**, 2135-2136 (1968).
6. B. Liedberg, C. Nylander, I. Lundstrom, "Surface plasmon resonance for gas detection and biosensing," *Sens. Actuators B* **4**, 299-304 (1983).
7. J.L. Melendez, R. Carr, D. U. Bartholomew, K. A. Kukanskis, J. Elkind, S.S. Yee, C. E. Furlong, R.G. Woodbury, "A commercial solution for surface plasmon sensing," *Sens. Actuators B* **35**, 212-216 (1996).
8. L.M. Zhang, D. Uttamchandani, "Optical chemical sensing employing surface plasmon resonance," *Electron. Lett.* **23**, 1469-1470 (1988).
9. A. V. Kabashin, P. I. Nikitin, "Interferometer based on a surface-plasmon resonance for sensor applications," *Quantum Electron.* **27**, 653-654 (1997).
10. A.V. Kabashin, P.I. Nikitin, "Surface plasmon resonance interferometer for bio- and chemical-sensors," *Opt. Commun.* **150**, 5-8 (1998).

11. A.N. Grigorenko, P.I. Nikitin, A.V. Kabashin, "Phase Jumps and Interferometric Surface Plasmon Resonance Imaging," *Appl. Phys. Lett.* **75**, 3917-3919 (1999).
12. S. Shen, T. Liu, and J. Guo. "Optical Phase-Shift Detection of Surface Plasmon Resonance," *Appl. Opt.*, **37**, 1747-1751 (1998);
13. A. G. Notcovich, V. Zhuk, and S. G. Lipson, "Surface plasmon resonance phase imaging," *Appl. Phys. Lett.* **76**, 1665-1667 (2000).
14. H. P. Ho, W.W Lam, "Application of differential phase measurement technique to surface plasmon resonance sensors," *Sens. Actuators B*, **96**, 554-559 (2003).
15. C. M. Wu, Z. C. Jian, S. F. Joe, L. B. Chang, "High-sensitivity sensor based on surface Plasmon resonance and heterodyne interferometry," *Sens. Actuators B* **92**, 133-136 (2003).
16. S. Y. Wu, H. P. Ho, W. C. Law, C. Lin, and S. K. Kong, "Highly sensitive differential phase-sensitive surface plasmon resonance biosensor based on the Mach-Zehnder configuration," *Opt. Lett.* **29**, 2378-2380 (2004).
17. A. K. Sheridan, R. D. Harris, P. N. Bartlett, and J. S. Wilkinson, "Phase interrogation of an integrated optical SPR sensor," *Sens. Actuators B* **97**, 114-121 (2004).
18. R. Naraoka, K. Kajikawa, "Phase detection of surface plasmon resonance using rotating analyzer method," *Sens. Actuators B*, **107**, 952-956 (2005).
19. P. Chiang, J. Lin, R. Chang, S. Su, and P.T. Leung, "High-resolution angular measurement using surface-plasmon-resonance via phase interrogation at optimal incident wavelengths," *Opt. Lett.*, **30**, 2727-2729 (2005).
20. S. Patskovsky, A.V. Kabashin, M. Meunier, J.H.T. Luong, "Properties and Sensing Characteristics of Surface Plasmon Resonance in Infrared Light," *J. Opt. Soc. Am A* **20**, 1644-1650 (2003).
21. S. Patskovsky, A.V. Kabashin, M. Meunier, J.H.T. Luong, "Surface Plasmon Resonance Sensor on a Silicon Platform," *Sens. Actuators B* **97**, 409-414 (2004).
22. P. Schiebener, J. Straub, J. M. H. Levelt Sengers, J. S. Gallagher, "Refractive index of water and steam as function of wavelength, temperature and density," *J. Phys. Chem. Ref. Data*, **19**, 677-717 (1990).
23. J. Rheims, J. Köser, T. Wriedt, "Refractive-index measurements in the near-IR using an Abbe refractometer," *Meas. Sci. Technol.* **8**, 601-605 (1997).

1. Introduction

Surface Plasmon Resonance (SPR) is known as a leading technology for label-free biosensing [1-4]. SPR sensors are generally implemented in the Kretschmann-Raether geometry to direct p-polarized light through a glass prism and reflect it from a gold covered prism facet in contact with analyte ambient liquid. The SPR effect produces a resonant transfer of energy from an incident photon to a plasmon over the metal/liquid interface, which is observed as a dip in the angular (spectral) dependence of the reflected light intensity. Biomolecular binding events on gold lead to an increase of the refractive index (thickness) of an organic layer on the metal film, resonantly changing conditions of SPR production and thus shifting angular [6,7] or spectral [8] position of the SPR dip. Such approach enables to avoid time-consuming labeling step and all reaction kinetics constants can be routinely obtained within minutes.

It has been recently found that the detection limit of the method can be improved by up to two orders of magnitude by monitoring phase characteristics of light reflected under SPR condition [9-11]. Such improvement was due to the fact that the phase of light can experience a much steeper change across the plasmon resonance region, compared to the intensity. However, the experimental realization of such sensitivity is not trivial because of instrumental and other noises. Most groups use a SPR interferometry [9-19], in which information on phase is extracted optically from spatial interference pattern, formed by interfering signal and reference (non-affected by SPR) beams, or SPR polarimetry (see, e.g., [20,21], analyzing the polarization state of light with p and non-affected s-component. Although these approaches provide a significant upgrade of sensitivity of the method and a possibility of efficient imaging, the dynamic range of measurements still needs to be improved.

In this paper, we describe a novel polarimetry-based scheme, which combines high phase sensitivity with wide dynamic range, and utilizes a much simpler instrumental arrangement.

2. Experimental setup and instrumental methodology

A schematic diagram of the proposed method is shown in Fig. 1. A 40mW laser diode operating at a wavelength of 780 nm is used as the light source. The light is passed through a quarter-wave plate and a polarizer to obtain a 45 deg. linearly polarized beam. The beam is

then directed through a custom-made prism (F2 glass) and a thin glass slide, which is in immersion contact with the prism, to be reflected from a gold covered glass slide facet in contact with an aqueous medium. The angle of light incidence on the gold surface is selected to produce SPR coupling and excite surface plasmons over the gold/liquid interface. The SPR effect is accompanied by a drastic decrease of intensity of the p-polarized component and a sharp jump of its phase, changing the total polarization state of light. A 90° deg. phase retarder is used after the sensor head to compensate the ellipticity (phase shift between the s- and p-components) caused by SPR. The beam is then passed through a photoelastic modulator (PEM), which is used to sinusoidally modulate p-component with the frequency $\phi = 42$ kHz. A polarizer (analyzer) is placed just after the PEM and oriented 45 deg. in front of the detector. Information on the phase-polarization state of light reflected under SPR is extracted by the examination of 2nd and 3rd harmonics of the modulated signal, with the help of a lock in amplifier. The SPR coupling block and optical parts were covered by a specially designed thermoisolation box to minimize thermal and inertial drifts.

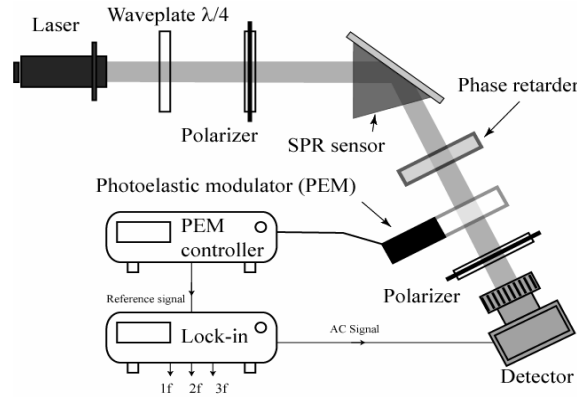


Fig. 1. Schematics of the experimental arrangement.

Changes of light polarization state in the proposed scheme can be considered using the Jones transformation matrix method. Here we imply that before PEM we have light of linear polarization, with the p-component over the plane XZ and the s-component over the YZ plane. Since the s-polarized light has no phase or amplitude changes under SPR, while p-polarized light experiences changes of both the amplitude A_x and the phase, the electric field of light after the SPR coupling block will be:

$$E_{SPR} = \begin{pmatrix} E_x \\ E_y \end{pmatrix} \text{ with } E_x = A_x \exp(i\phi_x + \alpha) \text{ and } E_y = A_y \exp(i\phi_y) \quad A_y = 1 \quad (1)$$

Here ϕ_x and ϕ_y are the initial phase components over x and y coordinates, respectively; α is a phase retardation under SPR. The modulation of the p-component with the frequency ϕ will lead to a relative phase retardation of this component $\psi = A_\psi \sin(\phi)$ and a resulting periodic-elliptical polarization of light. This can be described by the following Jones transformation matrix:

$$J_{PEM} = \begin{bmatrix} \exp(i\psi/2) & 0 \\ 0 & \exp(-i\psi/2) \end{bmatrix} \quad (2)$$

Then, the light passing through a polarizer with the rotation angle of θ will give rise to the following matrix:

$$J_p = \begin{bmatrix} \cos(\theta)^2 & \sin(\theta)\cos(\theta) \\ \sin(\theta)\cos(\theta) & \sin(\theta)^2 \end{bmatrix} \quad (3)$$

Finally, we need to take into account the phase retardation due to passing of light through a 90° deg. phase retarder by the retardation element J_{RET} , similar to J_{PEM} , with fixed retardation 90 deg. The final intensity after passing through these elements will be:

$$I = \bar{E} \cdot E \text{ where } E = J_p J_{PEM} J_{RET} E_{SPR} \quad (4)$$

Here, for the polarizer axis of 45 deg., we simplify the expression taking into account that:

$$\cos(\theta) = \frac{\sqrt{2}}{2} \text{ and } \sin(\theta) = \frac{\sqrt{2}}{2}.$$

Therefore, for the resulting intensity we have:

$$I = \frac{1}{2} A_x^2 + \frac{1}{2} - A_x \cos(A_\psi \sin(\varphi) + \alpha) \quad (5)$$

Using lock-in amplifier, we can decompose our final periodic signal into harmonics. Since our time domain signal is periodic and continuous, we can use the Fourier transform method to model the harmonics of a frequency spectrum. Thus, for first three harmonics we have:

$$F1 = 2 \cdot A_x \cdot J_1(M) \cdot \cos(\alpha) \quad (6)$$

$$F2 = 2 \cdot A_x \cdot J_2(M) \cdot \sin(\alpha) \quad (7)$$

$$F3 = 2 \cdot A_x \cdot J_3(M) \cdot \cos(\alpha) \quad (8)$$

where J_n are Bessel functions and M is equal to A_ψ . Despite almost similar equations for the three harmonics, their response will be different due to the dependences of the Bessel functions on the PEM modulation amplitude. Fig. 2 presents signals of the three harmonics as a function of the phase retardation α for two example modulation amplitudes A_ψ : $\pi/4$ (a) and $\pi/2$ (b). One can see that the 1st harmonics is much more sensitive to variations of α when the modulation amplitude A_ψ is equal to $\pi/4$, while the response of the 3rd component becomes predominant at $\pi/2$. In general case, the optimization of responses for different harmonics can be performed using the dependence of Bessel functions on the modulation amplitude, shown in Fig. 2 (c). Here, signals of the 1st, 2nd and 3rd harmonics have the Bessel functions of $J_1 = 0.582$, $J_2 = 0.486$ and $J_3 = 0.434$, and reach their maximal sensitivity at the modulation amplitudes of 51° deg., 85° deg. and 121° deg., respectively, while the 1st and 3rd harmonics have almost similar response under 90° deg. It is known that the use of the 2nd or 3rd harmonics is generally preferable compared to the 1st one due to a possibility of much easier filtering of external noises by lock-in technique. Therefore, in our tests we mainly used high harmonics signals.

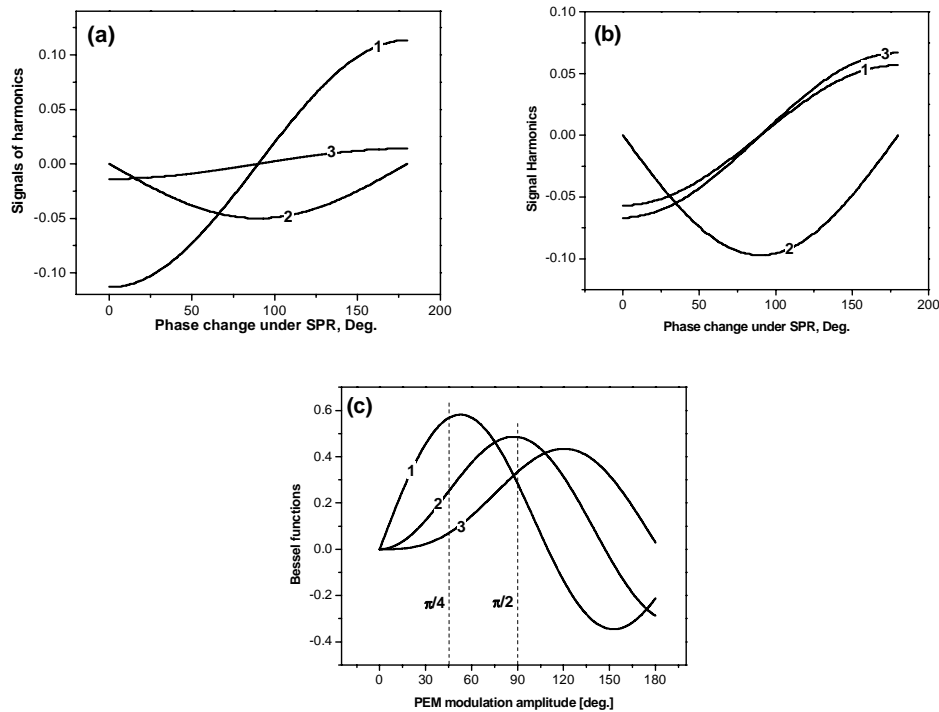


Fig. 2. Responses of 1st, 2nd and 3rd harmonics to phase changes $\Delta\alpha$ under the modulation amplitude of $\pi/4$ (a) and $\pi/2$ (b); (c) Dependence of Bessel functions on the PEM modulation amplitude.

Figure 3 shows typical SPR reflectivity and phase curves (a), as well as a simulation of the responses of phase and intensity of light, reflected under SPR, to changes of the ambient refractive index (b). These plots were obtained using Fresnel's formulas for a multi-layer system. Details on the model can be obtained in [22,23]. As shown in the Fig. 3, the phase can demonstrate much better sensitivity compared to the intensity, suggesting a possibility for a significant improvement of the sensitivity of the SPR technology. The domination of the phase sensitivity over the intensity one becomes especially remarkable under ultra-small refractive index (RI) variations, though the realization of such sensitivity requires a good optimization of the thickness of the gold film [9-11]. However, the dynamic range of phase measurements remains much narrower compared to that for the intensity.

In the proposed scheme, we use 2nd and 3rd harmonics to control the response of the system to refractive index change. This approach enables us to simultaneously take advantage of a high sensitivity and wide dynamic range, given phase and intensity measurements, respectively. Indeed, the 2nd and the 3rd harmonics represent a mixed response of phase and intensity, while their relative contribution can be optimized by choosing the modulation amplitude in accordance with Fig. 2c. We set the modulation amplitude at $\pi/2$ to maximize the sensing response of the 3rd harmonics and have a relatively good 2nd harmonics response.

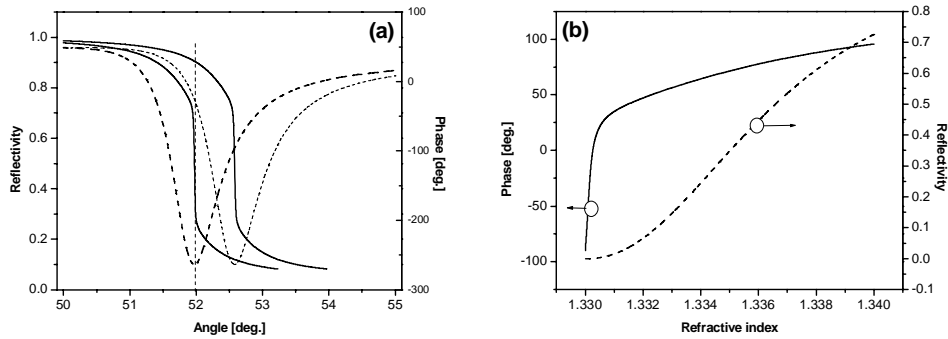


Fig. 3. (a) Angular reflectivity curves of intensity (dotted lines) and phase (solid ones) for different values of the refractive index; (b) Phase and intensity of light reflected under SPR as a function of the refractive index.

A simulation of the responses of these harmonics to RI change is shown in Fig. 4. Here, we show the contributions of phase and intensity (polarization) components in the combined signal of the 2nd and the 3rd harmonics. One can see that the control of the 2nd harmonic is effective only for relatively small RI changes. In this case, the sensitivity appears to be very high due to the prevailing contribution of the phase component. However, the dynamic range of the 2nd harmonics appears to be rather limited since the signal of this harmonic changes the polarity of its response under certain value of RI change (Fig. 4b). As shown in the Fig. 4, such a change of polarity is related to a competition of the phase and the intensity components, which make contributions of opposite polarities in the combined signal. In contrast, the 3rd harmonic shows much more promising sensing characteristics. First, for small RI variations it provides an ultra-sensitive response due to properties of its phase component (Fig. 4a). Then, under large RI variations, the intensity component prevails leading to a wide dynamic range of measurements. As a result, 3rd harmonic signals combine high phase sensitivity with a wide dynamic range of the intensity interrogation. It should be noted that a relative wideness of the dynamic range for the 3rd and 2nd harmonics is determined by the initial phase relation given by the phase retarder. In fact, the full pre-compensation of the phase shift by the adjustable retarder before introducing a small refractive index change to the system can lead to the opposite tendency for a wider dynamic range of the 2nd harmonic compared to the 3rd one. To verify the validity of the above theoretical analysis and draw conclusions, we carried out various tests for the newly introduced SPR polarimetry scheme. The results of these tests are described in the next section.

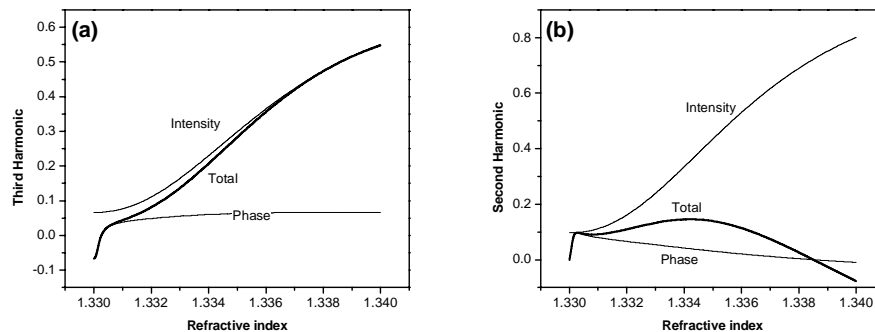


Fig. 4. Integral signals of the 3rd (a) and the 2nd (b) harmonics, as well as phase and intensity components of the signals, as a function of the refractive index.

3. Results

To estimate the sensitivity of the system, we examined the response of the 2nd and the 3rd harmonics when liquids with different refractive indices were brought into contact with the gold film. For these tests, we used glass slides with 50nm of gold film from PLATYPUS TECHNOLOGIES. In this chip, the thickness of the gold film is well optimized to provide a sharp jump of the phase of light reflected under SPR. Using a peristaltic pump, we introduced solutions of water with different concentrations of Glycerine. Knowing the difference of refractive indices of Glycerine and water, we could calibrate and determine the detection limit of our system. Fig. 5 (a,b) show responses of the 2nd and the 3rd harmonics when glycerine of a progressively increasing concentration was added to water.

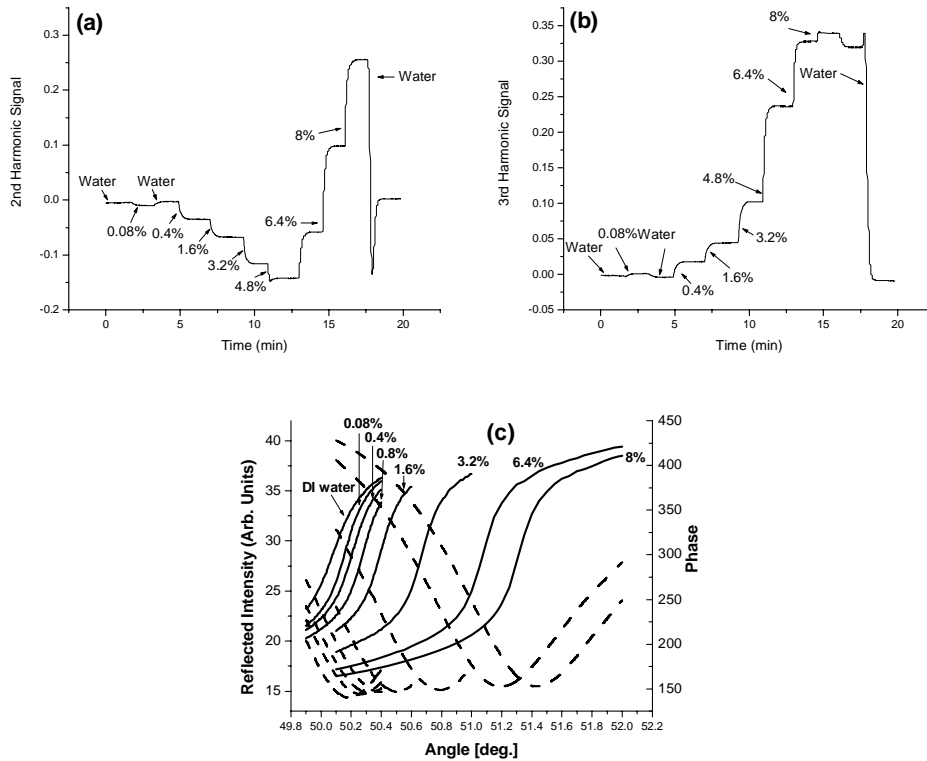


Fig. 5. Responses of the 2nd (a) and the 3rd (b) harmonics to the variation of the concentration of Glycerin in water; (c) Ellipsometry data: Angular dependence of the intensity (dashed line) and phase (solid line) on the concentration of glycerin in water.

One can see that both channels were able to easily detect even relatively small variations of glycerine concentration (0.08%), corresponding to the refractive index change of $1.1 \cdot 10^{-5}$. Larger variations of glycerine concentration were accompanied by a proportional change in signals of the two harmonics. Here, the signal from the 2nd harmonic experienced a change of the response polarity at some concentration of glycerine (8%). In fact, this change of polarity was consistent with our previous theoretical analysis, describing the evolution of the phase and the intensity components, as well as their combined signal. Indeed, as we showed earlier (Fig. 4a), this response polarity switch is explained by a relative contribution of the intensity component, which has the opposite response polarity compared to the phase one and becomes predominant at a certain concentration of glycerine. Fig. 5c depicts angular dependences for the reflectivity (dashed lines) and the phase (solid lines) under the same step changes of the

glycerine concentration. These dependences were obtained using a variable angle spectroscopic ellipsometer (Woollam VASE® ellipsometer, J.A. Woollam, Lincoln, NE), which made possible an extremely high precision of angular measurements (0.005 deg). As demonstrated in the Fig. 5, the phase experienced a sharp jump under SPR, confirming results of our theoretical calculations, shown in Fig. 3a. The phase and the reflectivity curves progressively shifted as the concentration of glycerin was changed. However, it can be easily found that under the fixed incidence angle, the phase provided a much stronger response to the RI change than the intensity, which is in agreement with previous studies of phase-sensitive SPR schemes [9-19]. Knowing the response of the 2nd and the 3rd harmonics and the corresponding response of the phase (Fig. 5 a-c), we can calibrate our system for small RI changes, when signals of the 2nd and the 3rd harmonics are almost purely phase. Results of such calibrations, shown in Fig. 6, indicate that both harmonics had almost a linear response to phase variations, while the sensitivities of these components were comparable.

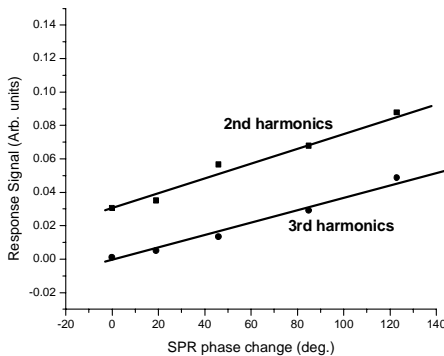


Fig. 6. Calibration curves for responses of the 2nd and the 3rd harmonics as a function of the SPR phase change.

To determine the detection limit of our experimental setup, we examined responses of the two harmonics under very small changes of refractive index. In this test, water was replaced by 0.005% of glycerine, corresponding to a refractive index change of $5.5 \cdot 10^{-6}$. Examples of the 2nd and the 3rd harmonics responses to such replacement are given in Fig. 7. One can clearly see that the replacement of water by glycerine led to a significant change of signals of both harmonics. In particular, the signal from the 3rd harmonic changed its value by 0.00768 units. As one can see from Fig. 7, such a change was still far from the detection limit of the system. To estimate this detection limit, we measured the level of noises in the system by pumping pure water in the sensor head for a period of 30 minutes. We found that the signal fluctuation does not exceed 4×10^{-4} units. Thus, we can conclude that the calculated detection limit of our setup of about 2.89×10^{-7} in terms of refractive index units (RIU). This sensitivity is at least 50-times better than the one in conventional SPR configurations employing the intensity as the main signal parameter [2-8]. Note that the measured value of the detection limit does not represent the physical limit given by phase characteristics (as it was shown in [9,10,16], the phase sensitivity can be lower than 10^{-8} , if SPR production conditions are well optimized), but is related to a relative predominance of the signal over noises in our experimental setup. We reason that in our case these noises were mainly related to laser power and temperature drifts. In particular, in the absence of a system for an active thermal stabilization, the latter drift could affect the value of the refractive index of analyte solutions (refractive index drift), increasing the detection limit of our measurements. It is clear that the mentioned drifts can be drastically reduced by optimizing the system design. For example, the power drift can be minimized by using a high-precision stabilized laser, while temperature drifts can be decreased by either active thermostating of the system or using differential

schemes. This is confirmed by results of previous studies (see, e.g., [16]), suggesting that even simple measures on the optimization of the system make possible a drastic decrease of noises.

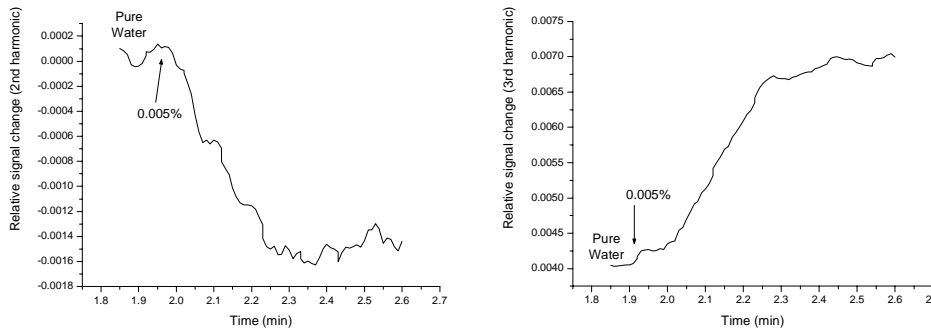


Fig. 7. Response of the 2nd and the 3rd harmonics to the variation of the concentration of Glycerine by 0.005% in water.

As it was concluded from calculations (Fig. 4), the 3rd harmonic must have a much wider dynamic range compared to the 2nd harmonic. To verify this conclusion, we measured the RI dependence of the signal of the 3rd harmonic under wide variations of the refractive index. As shown in Fig. 8, the signal really does not show any sign of saturation and can monitor RI changes until 10^{-2} RIU. We believe that such a wide dynamic range of measurements was due to advantages given by a simultaneous contribution of the phase and the intensity components. The phase component is predominant under small RI changes (normally below 10^{-4} RIU) providing an ultra-high phase-based sensitivity. In contrast, the intensity starts to prevail when phase saturates, i.e. under relatively large RI changes (above 10^{-4} RIU). Such a combination of contributions of the two components results in a continuous sensitive response of the integral 3rd harmonic signal. It is interesting that the 3rd harmonic signal demonstrates a close-to-linear dependence with respect to refractive index changes. This is a pleasant surprise, taking into account the rather complex nature of the response of this component.

As an example of biosensing applications of the proposed scheme, we used a reaction of avidin – biotin binding, which is frequently used to calibrate SPR biosensors. In this particular test, we used the 3rd harmonics to control the signal, while before the injection of biological substances gold was in contact with PBS buffer solution, as shown in Fig. 9. First, we injected 0.1 mg/ml of avidin, which is known to unspecifically bind with gold. This binding led to an immediate increase of the 3rd harmonic signal until its saturation, corresponding to a complete coverage of the gold surface. To wash unbound and weakly attached avidin, we injected PBS buffer, which led to a certain decrease of the signal. The re-injection of avidin led to restoration of the signal, corresponding to complete gold covering, while the secondary injection of PBS led to a much weaker decrease of the signal due to removal of some unbound avidin molecules. A subsequent injection of biotin caused its aggressive binding to avidin, and consequently to an increase of the thickness of the biological film on gold, which, in turn, resulted in an increase of the integral 3rd harmonic signal. It is interesting that a temporary cease of biotin supply and a subsequent injection of PBS did not lead to any decrease of the signal, as it took place in the case of pure avidin. In contrast, the signal continued to rise at the first moments of the PBS injection. Such behavior is apparently related to the fact that the avidin-biotin interaction is extremely strong and not easy to break. Therefore, the injection of PBS instead of detaching biotin from avidin washed its molecules from the walls of flow injection system, leading to a further increase of the integral signal. A subsequent injection of biotin led to a saturation of the signal corresponding to complete avidin-biotin binding, while further injection of PBS could not change the signal. It is important that our scheme enabled to follow the course of interactions in real time and resolve all kinetics constants. As shown in

the Fig. 9, every reaction or process (Gold-avidin; gold-avidin-PBS; avidin-biotin) has its own kinetics constant, describing the intensity of interaction. In fact, a routine ultra-sensitive determination of these constants is one of major advantages given by the SPR technology over fluorescent labeling methods.

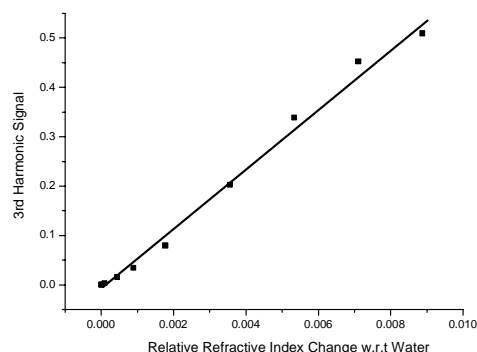


Fig. 8. Response of the 3rd harmonic as a function of the refractive index change.

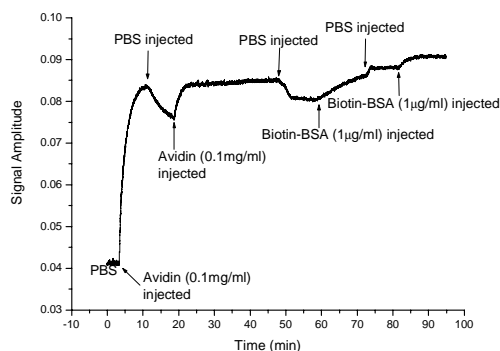


Fig. 9. Response of the 3rd harmonics to the reaction of avidin-biotin binding.

4. Conclusions

We have introduced a novel phase-sensitive SPR polarimetry scheme, which uses temporal modulation of the mixed-polarized beam reflected under SPR, by a photo-elastic modulator, and subsequent analysis of the 2nd and the 3rd harmonics of modulated frequency. We show that the proposed configuration has a much lower detection limit to refractive index (thickness) change in thin films, compared to conventional intensity-sensitive SPR. This method enables to keep a wide dynamic range of measurements, which is normally impossible or difficult with phase-sensitive SPR schemes. The proposed scheme has been successfully applied to follow a reaction of avidin – biotin binding on gold surface.

Acknowledgments

We acknowledge the financial contribution from the Natural Science and Engineering Research Council of Canada. Partial support from the John R. Oishei Foundation and the Center of Excellence in Bioinformatics and Life Sciences at the University at Buffalo is also acknowledged.